UNCERTAIN ESTIMATION OF SUBSURFACE TEMPERATURE AWAY FROM THE BOREHOLE USING MAGNETOTELLURIC INVERSIONS

Alberto Ardid[1], David Dempsey[1], T. Bertrand[2] and Rosalind Archer[1]

[1]University of Auckland, Auckland, New Zealand

[2]GNS Science, Upper Hutt, New Zealand

aard708@aucklanduni.ac.nz

Keywords: *Geothermal field, magnetotelluric, joint inversion, temperature distribution*

ABSTRACT

Although the magnetotelluric (MT) method has been used in geothermal exploration for some decades, there remain deficiencies in integrating resistivity data with other relevant variables and information, e.g., contemporary reservoir temperature, clay alteration, permeability and porosity. Here, we focus on the relationship between temperature and resistivity, specifically through the formation of clay minerals. We develop a methodology to extrapolate subsurface isotherms away from wellbore for which there is a temperature log. To do this, we use the resistivity distribution estimated from MT inversion assuming a correlation between shallow (clay) resistivity anomaly and clay formation temperatures. For the synthetic problem studied here, our method constrains isotherms and clay cap boundary, with uncertainties, up to 2km from a well. Our long term goal is to improve understanding of the relationship between resistivity and temperature, provide a method to image temperature away from boreholes, and develop methods to inform and validate reservoir models.

1. INTRODUCTION

In geothermal exploration, one of the primary goals is to elucidate the subsurface temperature distribution. This is usually investigated by direct measurements in wellbores, however, these can be difficult to extrapolate away from the well. Geophysical methods can fill in some of these gaps as they provide an inferred view of large volumes of the subsurface, suggesting constraints on rock physical properties like electrical resistivity. If these properties could be linked to direct measurements in wells, then this could provide a basis to constrain any extrapolation.

Joint inversions are methodologies that aim to integrate information revealed by two properties to achieve a better understanding of a certain quantity. For example, electrical resistivity has been combined with seismic velocity to correlate geological structures (Mellors et al., 2015; Moorkamp et al, 2007) allowing lithological classification (Gallardo and Meju, 2007), jointly inverted with temperature to estimate permeability (Munoz et al., 2010) and with estimated densities to reveal deep geological structures (Hautot et al., 2007: Santos et al., 2006: Jegen et al. 2009). Dempsey et al. (2016), in a synthetic approach, developed a method to jointly invert magnetotelluric (MT) survey data and downhole temperature profiles to infer the subsurface temperature distribution. Although disadvantaged by simple (empirical) mathematical correlations, the approach was nevertheless able to estimate some general features of the original temperature distribution.

This study develops a new approach to infer isotherms and clay cap depth in a geothermal field, using temperature data in a well and electrical resistivity from an MT inversion. Following Dempsey et al. (2016), we recreated the condition of a geothermal field from a synthetic approach, characterized by a low resistivity anomaly overlying the main upflow. This anomaly is assumed to be indicative of a highly conductive clay, smectite, resulting from hydrothermal alteration that dominates within a specific temperature range. We extend the joint inversion to consider physical constraints on temperature and heat transport, and to capture and visualize uncertainties in the input data and inversion.

2. GOING FORWARD: TEMPERATURE AND RESISTIVITY MODEL

In this section we describe how we simulate MT observations above a 2D synthetic geothermal field whose resistivity structure reflects a simple hydrothermal alteration model under natural state temperatures.

Following O'Sullivan and O'Sullivan (2016), the temperature distribution $T = T(y, z)$ in a generic geothermal upflow (Fig. 1) is simulated using the AUTOUGH2 software. The simulation models heat and mass transport in a convective hydrothermal cell, employing a simple representation of a geothermal field based on a single up-flow zone. We denote T as the 'true' temperature distribution. In subsequent steps, temperature data from 'wells' for the joint inversion is obtained from the true temperature distribution as profiles $T^i(y^i, z)$.

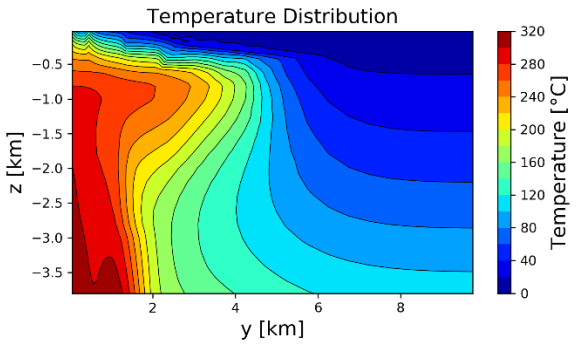

Figure 1: Synthetic natural state temperature model from AUTOUGH2. Black contours are isotherms. Upflow centered at y=0.

A synthetic 2D resistivity model is calculated using a simple alteration model that assumes rock resistivity is a function of natural state temperature. In practice, resistivity will be controlled by variations in other physical parameters like

porosity, permeability, fluid salinity and conductivity of the rock matrix, which has potentially been hydrothermally altered. We approximate the formation of conductive smectite clay using a band smoothed boxcar function $\Gamma(T,\phi)$ (Figure 2) where $\phi = [t_m, t_w, t_{wl}, t_{wr}, \rho_a, \rho_o]$ is a vector of model parameters (see Dempsey et al., 2016, for details). For each block temperature in the AUTOUGH2 model, an associated resistivity is calculated. The modelled resistivity at that location is assigned by sampling a normal distribution centered on $\Gamma(T,\phi)$. This introduces heterogeneity, but also an element of uncertainty when inverting to find the occurrence temperature of smectite alteration. The result is a 'true' resistivity distribution, $\rho(y,z) = \Gamma(T(y,z),\phi)$ (Figure 3). Alteration model parameters and range of resistivity for each temperature are based on Browne and Ellis (1970), Browne (1978), Steiner (1953), Morrison (1997) and Gunerson (2000).

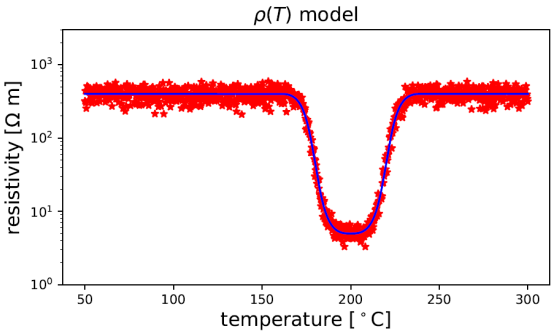

Figure 2: Alteration model (function) that computes rock resistivity in terms of rock temperature. The blue line denotes the boxcar function. Red dots denote temperatures assigned after the distribution in the established range.

From the 2D true resistivity distribution, $\rho(y,z)$, an MT surface response is computed at certain station locations at the Earth's surface. The apparent resistivity, ρ_{app}, is assumed to be measured at discrete periods, ω, and the response varies between stations. In this study, we used a station spacing of 500 m out to 10 km from the centre of the up-flow and a period bandwidth of 10^{-3} to 10^{3} s. The forward MT response is computed using the MT inversion code ModEM (Modular system for Electromagnetic inversion; Kelbert et al., 2014) operating in forward mode.

3. GOING BACKWARDS: JOINT INVERSION

We wish to estimate subsurface temperatures, $T_{est}(y,z)$, using MT observations, ρ^i_{app}, and well temperature observations $T^w(y^w,z)$. For the temperature observations, we consider a single well located in the centre of the up-flow zone, $y^w = 0$ km, and assume that an equilibrated temperature has been measured to a depth of 1 km.

The major steps to estimate the temperature distribution are: (1) invert apparent resistivity observations, ρ_{app}, to obtain an estimated resistivity distribution of the subsurface $\rho_{est}(y,z)$; (2) model a relationship between well temperature measurements, T^w, and the resistivity estimated at the same profile, $\rho^w_{est}(y^w,z)$; (3) extrapolate temperature away from the well employing, ρ_{est}, from the relationship built.

3.1 MT inversion

Synthetic MT observations, ρ_{app}, are inverted using ModEM (Kelbert et al., 2014) to infer the electrical resistivity distribution. Such inversions are typically ill-posed problems, and some form of regularization is necessary to obtain a unique solution. As a result, the inferred distribution, ρ_{est}, is not likely to match the "true" distribution, ρ, particularly when there are sharp boundaries in the true resistivity distribution; the regularization algorithm will tend to smooth these out.

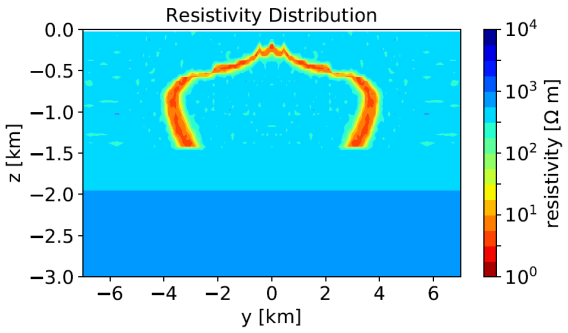

Figure 3: True resistivity distribution.

Figure 4 shows the results of the inversion, ρ_{est}. Although smoothing effects can be noticed, the inversion recovers the main aspects of the true resistivity model capturing the size, some features of shape and resistivity properties of the low resistivity anomaly (clay cap above the up-flow zone; Figure 3).

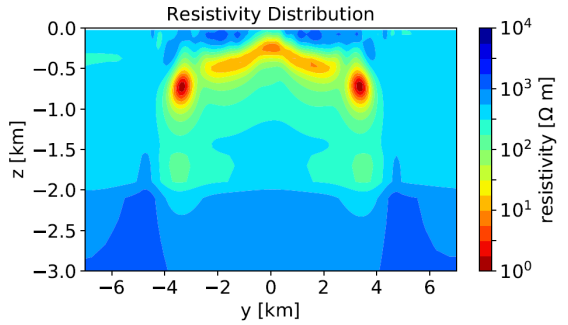

Figure 4: Inferred resistivity distribution obtained by inversion of the MT observations.

If the inversion were perfect ρ_{est} would match ρ_{true}, and if the model parameters ϕ of the alteration process function Γ were also known, then we could infer aspects of T by applying $\Gamma^{-1}(\rho_{est},\phi)$. In practice, ρ_{est} approximates the true values and we have only basic knowledge of Γ (dominant interval of temperature of where alteration occurs t_m, t_w and range of resistivities associated ρ_a, ρ_o (Figure 2). Instead then, we shall establish two approaches, based on mathematical and physical relationships, to link temperature and resistivity at the borehole, and then extrapolate this relationship to other parts of the field.

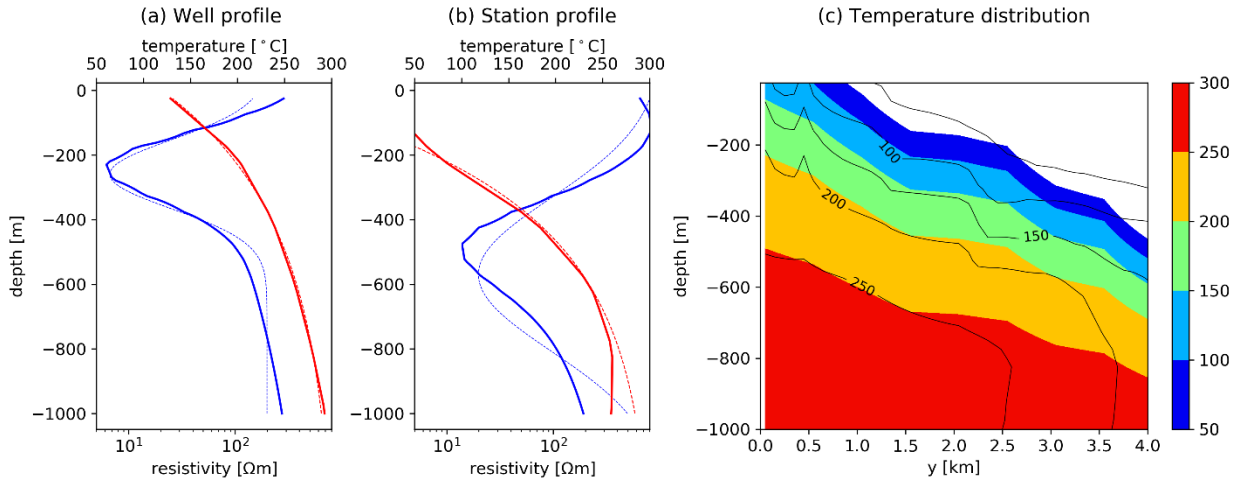

Figure 5. Summary of joint inversion for Approach 1 (Section 3.2). (a) Temperature measurements (red line) and corresponding values of resistivity (blue line) for a well located in the centre of the up-flow. Fitting curves are indicated by dash lines. (b) For a station located at 2 km, values of estimated resistivity (blue line), best-fit normal distribution (dash blue line), true temperature profile (red line) and predicted temperature extrapolated from the correlation in (a). (c) Comparison between inferred (filled contours) and true temperature distribution (black isotherms).

3.2 Relationship ρ↔T: Approach 1

This section replicates the approach and results of Dempsey et al. (2016), which uses an empirically derived correlation between inferred resistivity and observed temperature.

Figure 5a shows the resistivity and temperature profile, ρ_{est}^{w} and T^{w}, in a well centred at the middle of the up-flow zone. We approximate $log(\rho_{est}^{w})$ using a normal distribution and T^{w} using a simple 1D heat transport model (Bredehoeft and Papadopoulos, 1965) with a convective shape (slight slope near the surface that increases with depth):

$$T = (T_{max} - T_{min})\frac{exp\left(\beta\frac{z - z_{min}}{z_{max} - z_{min}}\right) - 1}{exp(\beta) - 1} + T_{min}, \quad (1)$$

where $[T_{min}, T_{max}, z_{min}, z_{max}]$ are boundary conditions and β captures the relative strength of conductive versus convective heat transfer. We assume that the 1D model is a good representation of heat flow throughout the up-flow zone, however, the model will not perform so well in regions where flows are dominantly horizontal.

Extrapolation follows as: (i) find the best normal distribution approximation at ρ_{est}^{j} (inferred resistivity above location j); (ii) identify the depth offset between the centre of mass of ρ_{est}^{j} and ρ_{est}^{well}; and (iii) generate T_{est}^{j} (temperature profile at location j) by translating the approximation in T^{w} upward or downward accordingly.

Figure 5b shows ρ_{est}^{j} and temperature estimation, T_{est}^{j}, compared against the true value, T^{j}, for a station 2.0 km from the well. Figure 5c applies the same method to estimate temperature up to 5 km from the well, which is sufficient to go beyond the edge of the clay cap.

3.3 Relationship ρ↔T: Approach 2

Here, we present a refinement of Approach 1 that introduces a more physically motivated resistivity-temperature correlation. Furthermore, the new approach allows for uncertainty to be incorporated.

We assume that the vertical resistivity profile at a given location can be approximated by a simple 3-layer model $\rho_{3l}^{i}(y, z)$. Physically, these layers are intended to represent the clay cap and the unaltered rock above and below. The heat equation (1) is then modelled within each layer.

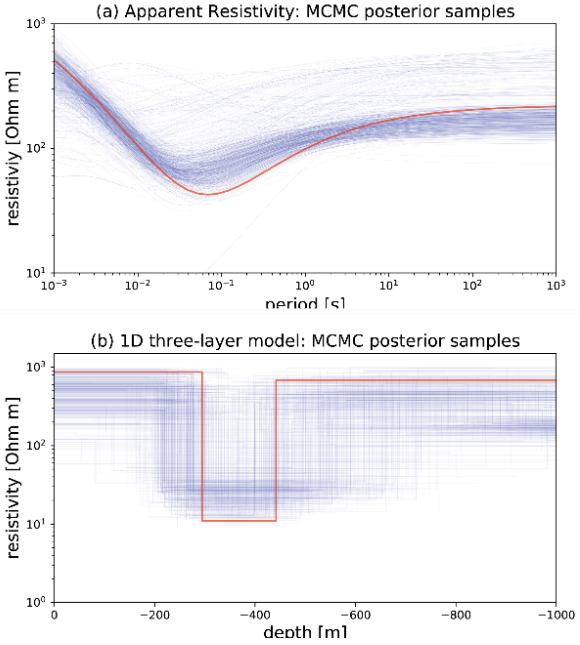

Figure 6: (a) Three-layer apparent resistivity models (blue lines) that approximately fit a surface response calculated from the inferred resistivity distribution (red line) for a station located 1 km away from the well. These models are derived from the posterior function of MCMC inversion (blue lines); (b) three-layer models generating the surface responses in (a). The best fit model is given by the red line.

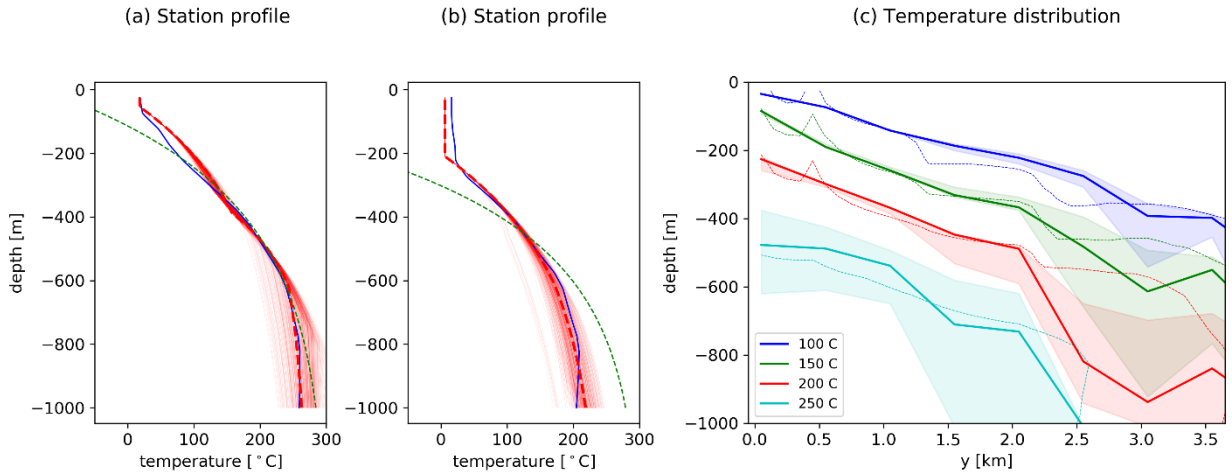

Figure 7. Summary of joint inversion for Approach 2 (Section 3.3). (a) and (b) show the true temperature profile (blue line), the profile estimated by Approach 1 (green line), and a series of profiles estimated by Approach 2 (red lines, best-fit is dashed) for stations located at (a) 1 and (b) 3.5 km away from the well. Red dash line shows the best fitting profile while other curves are are samples from the MCMC posterior function. (c) Comparison between isotherms estimated by Approach 2 and true ones (dash lines). Estimations are plotted with their associated uncertainty (envelopes bracket 5 and 95 percentiles).

Extrapolation proceeds by: (i) At the location of the well, determine the 3-layer resistivity model (layer thicknesses and resistivities), ρ_{3l}^{well}, that best approximates the surface response. (ii) For each layer of ρ_{3l}^{well}, determine a value β for the best-fitting a temperature profile (Eq. 1) to T^w, ensuring that T is continuous between layers. (iii) For a different vertical profile at location, y^j, away from the well, calculate a set of plausible 3-layer resistivity model, ρ_{3l}^j, that approximate ρ_{est}^j. (iv) For each possible resistivity profile, ρ_{3l}^j, generate a temperature profile using Eq. (1) and the layer β values determined in step (ii). Temperature boundary conditions at the layers are determined from T^w and ρ_{3l}^{well}.

The steps to calculate a three-layer resistivity model best approximating the surface response at particular location are: (i) calculate by forward modelling the 1D surface response, $\rho_{app}^{well}(\omega)$, using the inverted resistivity distribution $\rho_{est}^{well}(z)$. (ii) Invert, $\rho_{app}^{well}(\omega)$, using Markov-Chain Monte-Carlo (MCMC) to find parameters of the best-fit 1D three-layer resistivity model, $\rho_{3l}^{well}(z)$ (Figure 6). The advantage of MCMC is that it allows us to generate a posterior distribution over the parameters of the 3-layer model. This can then be sampled to generate multiple inversions consistent with the data, hence enabling quantification of the solution uncertainty.

Figure 7a shows estimated temperature profiles and the true value for two stations located at (y^j) 2.0 and 3.5 km distance from the wellbore. We applied the extrapolation at 500 m spacing up to 4.0 km distant from the wellbore. As the simulated well depth is only 1 km, we did not extrapolate beyond this depth. Vertical extrapolation would require a different approach to that developed in this study.

Figure 7c summarises the main features of the extrapolation showing estimated isotherms (with uncertainty) against the true values. Isotherm envelopes are built from 500 samples recovered from the MCMC inversion, plotting the median and 5%-95% percentile depths corresponding to each isotherm value.

4. DISCUSSION

Figures 7a and 7b compare extrapolated temperature profiles under the two approaches for stations 2.0 and 3.5 km away from the well. The true temperature is also shown. Although the normal approximation to the resistivity profile is weak for the first approach (Figure 5b), the temperature estimation is acceptable, recovering the main shape and values of the true curve. The second approach also provides a good estimate of the true temperature (Figure 7a). In contrast, Figure 7b shows the second approach is superior at estimating the true temperature that the first, which overestimates deep temperatures and underestimates shallow ones.

Within 2.5 km of the well, both approaches generate reasonable agreement with the true temperature distribution in the range 100-250°C. Beyond this distance, only Approach 2 recovers the deepening of the 200 and 250°C iosotherms. However, at 3 km – corresponding to an anomaly in the inverted resistivity distribution (Figure 4) - there is a substantial discrepancy in the temperatures recovered by Approach 2. This probably relates to the MT inversion struggling to recover the proper cap geometry at the transition from dominantly horizontal to dominantly vertical structure at around y=4 km. Complex cap geometries are likely to present a challenge in future studies.

Although both approaches do a reasonable job extrapolating temperature away from the borehole, Approach 2 has the advantages of being both physically motivated – using a 3-layer resistivity approximation as opposed to fitting an arbitrary function – and attaching uncertainty to its predictions. Therefore, its performance is likely to be greater in future studies where we explore more complex temperature, permeability and well patterns.

Figure 8 shows uncertain distributions for the inferred top and bottom boundaries of the clay cap as given by 3-layer model samples obtained from the posterior function. Knowledge of the bottom of this structure is particularly useful in drilling, when targeting the high temperature, permeable reservoir. Due to the diffusive nature of

penetrating electric fields, MT inversions tend to have less resolution with depth. This is reflected in the increased uncertainty in the depth to the bottom of the clay cap compared to the top. Nevertheless, our inversion captures the depth of the top and bottom of the cap out to 2 km from the upflow. At greater distances, the cap geometry changes and this is not properly captured by the inversion.

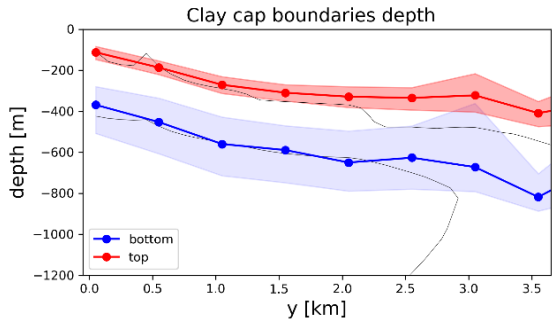

Figure 8. Estimated top and bottom boundaries for clay cap calculated from 3-layer model samples from the posterior function in the MCMC inversion (See Section 3.3) and true values (black lines).

In developing the presented methodology, we have had to make several assumptions. First, we have only considered a simple geothermal system with a single up-flow zone. Further we assume temperatures in the system are in a steady-state and that the alteration distribution reflects this. The clay alteration model we use assumes that rock resistivity is dominantly a function of temperature. In reality, resistivity will have a complex dependence on permeability, porosity, fluid composition, and other site dependent properties. Additionally, for the MT forward and inversion, we assume a 2D earth with no change in properties in out-of-plane dimension.

In implementing our joint inversion, there are three significant assumptions. First, in applying equation (1) to approximate vertical temperature profiles, we are implicitly assuming that heat transport is dominantly vertical throughout the up-flow zone. Second, we have assumed that a 1D three-layer resistivity model is an adequate representation of the first-order structure of a 2D system dominated by a conductive clay cap. Third, the relationship between temperature and resistivity sampled at the well is generally reflective of the relationship away from the well (i.e., extrapolation is valid). Although the assumptions are extensive, synthetic studies such as these offer a practical means to test their limits. However, in the future, application of the techniques to a well characterised field site will be essential to making further advances.

The introduction of model uncertainty has been considered in both the alteration model (Figure 2) and the fitting of 3-layer 1D models in Approach 2. Future work could also consider measurement error in the collection and processing of the MT surface response data as well as non-uniqueness inherent in the inversion algorithm.

5. CONCLUSION

We have developed a physically motivated methodology to integrate MT inversions and borehole temperature data for the goal of uncertain extrapolation of geothermal isotherms away from the wellbore. We have applied the methodology to a synthetic case study and compared its performance to another empirical approach. Over the long-term, our goals are to improve our understanding of the relationship between resistivity and temperature in the clay cap and our knowledge of the temperature distribution away from boreholes, thus giving an opportunity to inform and validate reservoir models.

The joint inversion we present is able to recover general features of a synthetic temperature distribution generated by a reservoir simulator. However, there are several areas where improvements and extensions could be made. By identifying new mathematical and physical correlations between the true resistivity and temperature profiles, a better fit in the extrapolated temperature could be achieved. It will also eventually be necessary to extend the study to consider 3D structure and incorporate more than one well, thus approaching a more realistic field case. We also need to study in more detail the alteration model, considering non-site dependent relationships. Furthermore, a global estimate of uncertainty is desirable, mainly by introducing MT modelling uncertainties. Finally, the usefulness of this joint inversion approach will be best assessed through application to a well-characterised field site.

ACKNOWLEDGEMENTS

The authors are grateful to Gary Egbert for providing access to the ModEM code used in this study.

REFERENCES

Bredehoeft, J. D., and I. S. Papadopulos (1965) Rates of Vertical Groundwater Movement Estimated from the Earth's Thermal Profile. Water Res. Res., 1, pp. 325-328.

Gallardo, L. A., and M. A. Meju (2007) Joint two-dimensional cross-gradient imaging of magnetotelluric and seismic traveltime data for structural and lithological classification: Geophysical Journal International, 170, 1–12.

Hautot, S., R. Single, J. Watson, N. Harrop, D. A. Jerram, P. Tarits, K. A. Whaler, and G. Dawes (2007) 3-d magnetotelluric inversion and model validation with gravity data for the investigation of flood basalts and associated volcanic rifted margins: Geophysical Journal International, 170, 1418–1430.

Jegen, M., R. Hobbs, P. Tarits, and A. D. Chave (2009) Joint inversion of marine magnetotelluric and gravity data incorporating 2 seismic constraints 3 preliminary results of subbasalt imaging off the Faroe Shelf: Earth and Planetary Sciences Letter, In Press.

Kelbert, A., N. Meqbel, G. D. Egbert, and K. Tandon (2014) ModEM: A modular system for inversion of

electromagnetic geophysical data. Comp. Geosci. 66, pp. 40-53.

Moorkamp, M., A. G. Jones, and D. W. Eaton (2007) Joint inversion of teleseismic receiver functions and magnetotelluric data using a genetic algorithm: Are seismic velocities and electrical conductivities compatible: Geophysical Research Letters, 34, 1–5.

Santos, F. M., P. Represas, and A. L. E. Sorady, (2006) Joint inversion of gravity and geoelectrical data for groundwater and structural investigation: application to the northwestern part of Sinai, Egypt: Geophysical Journal International, 165, 705– 718.

Mellors, R. J., A. Tompson, X. Yang, M. Chen, A. Ramirez, and J. Wagoner (2015) Stochastic Joint Inversion Modeling Algorithm of Geothermal Prospects. Proc. 40th Workshop on Geothermal Reservoir Engineering, Stanford, CA, USA.

Muñoz, G., K. Bauer, I. Moeck, A. Schulze, and O. Ritter (2010) Exploring the Groß Schönebeck (Germany) geothermal site using a statistical joint interpretation of magnetotelluric and seismic tomography models. Geothermics 39, pp. 35-45.

Browne, P. R. L., and A. J. Ellis (1970) The Ohaki-Broadlands hydrothermal area, New Zealand: Mineralogy and related chemistry. American Journal. of Science 269, 97-133.

Browne, P.R.L., (1978) Hydrothermal alteration in active geothermal fields. Annual Review Earth and Planetary Sciences 6, 229–250.

Dempsey D., J. O'Sullivan, and S. Pearson. (2016) Joint inversion of temperatures in a synthetic geothermal field using MT, clay alteration models, and geothermal reservoir simulation. 38th New Zealand Geothermal Workshop. 23-25 November, Auckland, New Zealand.

Gunderson, R., W. Cumming, U. Astra, and C. Harvey, (2000) Analysis of smectite clays in geothermal drill cuttings by the methylene blue method: for well site geothermometry and resistivity sounding correlation. Proc. World Geothermal Congr., KyushuTohoku, Japan, pp. 1175–1181

Morrison, K. (1997) Important hydrothermal minerals and their significance. Geothermal and Mineral Service Div., Kingston Morrison Ltd.